



# Structural control in micelles of alkyl acrylate-acrylate copolymers via alkyl chain length and block length

Özge Azeri<sup>1</sup> · Dennis Schönfeld<sup>1</sup> · Laurence Noirez<sup>2</sup> · Michael Gradzielski<sup>1</sup>

Received: 29 January 2020 / Revised: 18 April 2020 / Accepted: 18 April 2020 / Published online: 2 June 2020  
© The Author(s) 2020

## Abstract

Amphiphilic copolymers with poly (alkyl acrylate) as hydrophobic and poly (acrylic acid) (AA) as hydrophilic block have been synthesised. The alkyl chain was varied from butyl to dodecyl, thereby varying systematically the polarity of the hydrophobic block whose length was between 35 and 70, while the PAA block had ~ 100 units. Such relatively short amphiphiles should equilibrate quickly in aqueous solution, and their corresponding self-assembly properties were characterised by means of critical micelle concentration (cmc) determination. Detailed information regarding the aggregate structures was obtained by static light scattering (SLS) and small angle neutron scattering (SANS). This could be correlated with the molecular architecture of the copolymers and the degree of ionisation of the PAA block. Generally, it is found that the aggregation numbers become smaller upon fully charging the PAA head group and only for dodecyl acrylate really well-defined micellar aggregates are formed. This means that the extent of hydrophobicity of the alkyl acrylate block and its length determine in a clear fashion the propensity for micelle formation and the mass and aggregation number of the formed micelles.

**Keywords** Amphiphilic copolymers · ATRP · Polyacrylate · Self-assembly · Small angle neutron scattering

## Introduction

Amphiphilic block copolymers with a hydrophilic and a hydrophobic block are able to form micelles in aqueous solution and such systems have been studied to quite some extent due to the fact that there is an enormous richness in terms of combining different hydrophilic and hydrophobic copolymer blocks [1], for instance the hydrophilic block can be a polyelectrolyte [2, 3] or a nonionic water soluble polymer, like polyethylene oxide [4–6]. Such block copolymer micelles are interesting for a number of applications, such as drug delivery [7], in nanomedicine [8], or nanolithography [9]. Via

the length of the individual block, one can control the overall size of the aggregates, while their architecture (spherical, rod-like, locally lamellar etc.) depends mostly on the length ratio of hydrophilic and hydrophobic block [10–12]. Accordingly, not only micelles can be formed in aqueous solution but also vesicular structures or nanotubes [13]. The assembly properties can be rationalised by the packing parameter concept according to which the ratio of the volume  $v_h$  of the hydrophobic part and the product of interfacial area  $a_h$  (at the interface between hydrophobic and hydrophilic part of the molecule) and effective length  $L$  of the hydrophobic part determines the shape of the formed aggregates [14]. For  $p = v_h/(a_h \cdot L)$  smaller  $1/3$ , one expects for formation of spherical micelles, for  $1/3 < p < 1/2$  rod-like micelles and for larger  $p$  values locally planar structures, such as vesicles.

Quite frequently, such micelles are stimuli-responsive, for instance if the hydrophilic head group is a polycarboxylate or a polyamine which are switchable with respect to their charge by pH changes in the range of pH 5–9 [15, 16]. Another requirement is that the hydrophobic blocks should not be too long and be in a fluid state at the given temperature, as below the glass transition temperature, typically static micelles are observed [17]. For instance, for the case of polystyrene as hydrophobic block, no response to a solvent change was

---

**Electronic supplementary material** The online version of this article (<https://doi.org/10.1007/s00396-020-04663-y>) contains supplementary material, which is available to authorized users.

---

✉ Michael Gradzielski  
michael.gradzielski@tu-berlin.de

<sup>1</sup> Stranski-Laboratorium für Physikalische und Theoretische Chemie, Institut für Chemie, Technische Universität Berlin, 10623 Berlin, Germany

<sup>2</sup> Laboratoire Léon Brillouin CEA-CNRS, Université Paris-Saclay, 91191 Gif-sur-Yvette Cedex, France

observed [18]. Such responsiveness together with the ability to incorporate payloads of drugs makes block copolymer micelles also attractive as tunable delivery vehicles for nanomedicine applications, as reviewed recently [8, 19].

When considering block copolymer micelles for solubilisation and delivery purposes, it is very important to have a hydrophobic domain, whose polarity can be tuned often as interesting solubilisates (e.g. drug molecules) of intermediate polarity, and then the hydrophobic block has to be adapted to them in order to yield good solubilisation. Accordingly, we synthesised well-defined amphiphilic copolymers with poly alkyl acrylate as hydrophobic part, where the extent of hydrophobicity was varied via the length of the alkyl chain, and polyacrylic acid (PAA) as hydrophilic head group. Subsequently, their aggregation behaviour in aqueous solution was studied by means of scattering methods. The alkyl chain was changed from butyl (Bu) over hexyl (Hex) to dodecyl (Do), thereby systematically varying the extent of hydrophobicity. It might be noted that a similar system of poly(*n*-butyl acrylate)-*b*-poly (acrylic acid) has been studied before for longer PnBuA chains. In that study, quite monodisperse micelles have been reported that are relatively robust against changes of external parameters like pH or salinity [20].

In our investigation, the hydrophobic block was varied from 35 to 70 units in order to elucidate the effect of the block length (and thereby the degree of hydrophobicity) while keeping the length short in order to avoid the appearance of kinetically frozen micelles, as for instance they have been reported for longer poly(*n*-butyl acrylate) (PnBuA) micelles [21]. The copolymer micelles formed in aqueous solution were studied in structural detail by means of static light scattering (SLS) and small-angle neutron scattering (SANS) as a function of copolymer type and concentration. Besides hydrophobicity, pH-dependency was also investigated via changing the degree of ionisation  $\alpha$  of 0.2 to 1.0 (to ensure complete deprotonation of the polymer we worked here with an excess amount of NaOH, by adding 20% more than necessary for achieving the nominal value of  $\alpha = 1.0$ ).

## Materials and methods

### Materials

Toluene (> 99.5%) from Fluka, methyl-2-bromopropionate (2-MBP, 98%) and hexane from Aldrich, N,N,N',N'',N'''-Pentamethyldiethylenetriamine (PMDETA, 99%), hexyl acrylate (98%) and dodecyl acrylate (technical grade 90%) from Sigma-Aldrich and diethylether (> 99.5%) from Carl Roth were used as supplied. *tert*-Butylacrylate, *n*-butylacrylate and dichloromethane were gifts from BASF and used as supplied. Milli-Q water was produced by a Millipore filtering system. D<sub>2</sub>O was from Eurisotop (99.5% isotopic purity,

Gif-sur-Yvette, France) and sodium hydroxide (99%) and sodium chloride (> 99%) were obtained from Sigma-Aldrich. Silica (0.04–0.063 mm) from Merck was used for columns. Trifluoroacetic acid (> 99.9%) was from Roth.

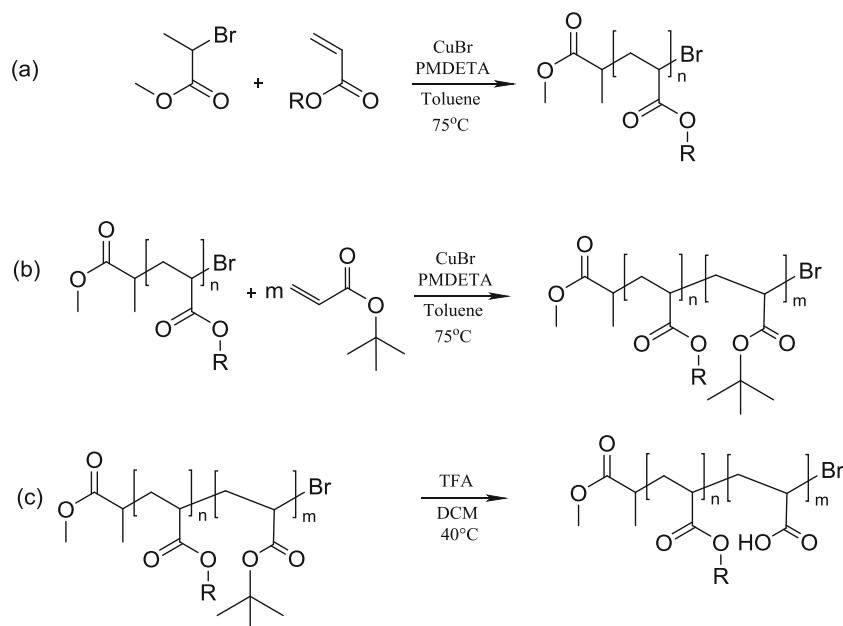
### Synthesis of polymers

The synthetic procedure was the same for all samples (depicted in Fig. 1), where one begins with the polymerisation of the first monomer to yield a macroinitiator for atom transfer radical polymerisation (ATRP). In the next step, this macroinitiator was used for further polymerisation of *tert*-butyl acrylate via the functional halide group that the polymer carries due to the chosen ATRP mechanism. The formed *n*-alkyl acrylate-*tert*-butyl acrylate block copolymer was an intermediate product that was transformed to the final product by selective hydrolysis of the *tert*-butyl groups, which was done by reacting with an excess of trifluoroacetic acid (TFA).

In particular, in a 100 ml single-neck flask with stirrer, Cu(I) Br (1.1 eq) and the *n*-alkyl monomer (20 or 40 eq) were weighted in. Subsequently, 40 ml toluene as solvent was added; the flask was closed with a septum and degassed while stirring for 20 min under nitrogen gas. After removal of the oxygen via bubbling with inert gas, first 2-MBP (1 Eq.) and then PMDETA (1.05 eq) were added into the reaction medium. The temperature of the oil bath was adjusted to 75 °C. The conversion was checked by means of <sup>1</sup>H-NMR. After about 24 h, the macroinitiator of reactive poly (alkyl acrylate) was ready (Fig. 1a). The intermediate block copolymer, consisting of poly (alkyl acrylate)-*b*-poly (*tert*-butyl acrylate), was synthesised in a one-pot reaction. First, *tert*-Butyl acrylate (100 eq.) was added into a 50 mL single-neck flask with stirrer and closed with a septum before stirring and degassing for 20 min. CuBr and toluene were placed in another 50 mL one-necked flask and degassed. PMDETA was injected into the flask with CuBr. After dissolving the CuBr owing to complexation of ligand and metal salt, the degassed *tert*-butyl acrylate and ligand-metal complex were transferred via cannula to the flask containing macroinitiator. The conversion of the reaction was checked via <sup>1</sup>H-NMR, and when the desired conversion was reached, the reaction was stopped by cooling down to ambient temperature and opening the flask. Next, the copper complex was removed by column chromatography with silica as a stationary phase and dichloromethane as eluent.

Finally, the hydrolysis of the *tert*-butyl group was performed with trifluoroacetic acid (TFA) for 96 h while stirring at 40 °C in dichloromethane to obtain a final product of polyacrylic acid. NMR was used to control the progress of the hydrolysis through checking to vanish the peak from the *tert*-butyl group. After 96 h, the reaction was stopped via cooling down the reaction medium. Excess amount of TFA was evaporated under vacuum, and the residue was washed with

**Fig. 1** Synthetic steps to prepare the poly (alkyl acrylate)-*b*-poly (acrylic acid) block copolymers by the ATRP procedure. **a** Polymerisation of the alkyl acrylate block ( $R = C_4H_9, Bu; C_6H_{13}, Hex; C_{12}H_{25}, Do$ ). **b** Polymerization of the *tert*-butyl acrylate block; intermediate product. **c** Hydrolysis of the intermediate product to yield the final product



hexane and then diethyl ether to get the final product. The obtained different types of block copolymers are depicted in Fig. 2.

The pH dependency of synthesised polymers was investigated via pH titration. A certain amount of block copolymer was dissolved in water and NaOH was added into the solution to deprotonate it completely. During the titration with 0.1 M HCl, the excess of NaOH was neutralised first and then polymer had become protonated. The degree of deprotonation  $\alpha$  was defined as follows:

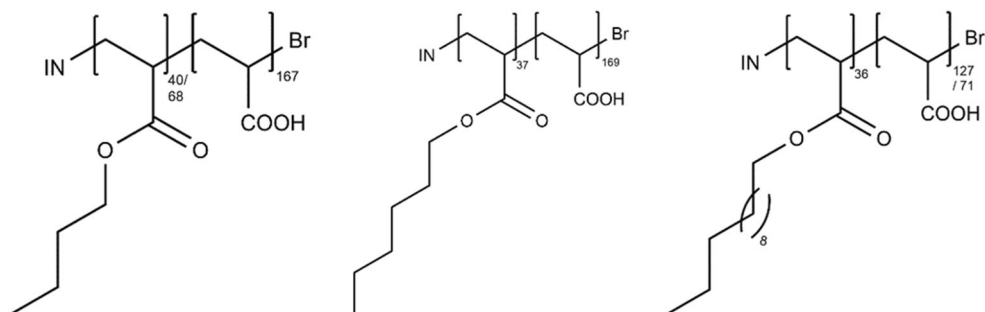
$$\alpha = \frac{n(OH^-)}{n(AA)}$$

where  $n(OH^-)$  are the total moles of added NaOH and  $n(AA)$  are the moles of acrylic acid units. This value for acrylic acid/the chargeable groups was used for the characterization of the synthesised polymers in further analysis.

### Characterization of the polymers

The above-synthesised copolymers were analysed with respect to their molecular composition. In a first step, this was

**Fig. 2** The different types of polymers synthesised as follows: poly (butyl acrylate)-*b*-poly (acrylic acid), poly (hexyl acrylate)-*b*-poly (acrylic acid) and poly (dodecyl acrylate)-*b*-poly (acrylic acid)



done by NMR on the intermediate product that still contains the *tert*-butyl acrylate (t-Bu) units, as here, the signal of the t-Bu groups yields just one sharp singlet, which can be well distinguished from the signals of the alkyl groups. These measurements were done in  $D_2$ -dichloromethane as solvent with a Bruker Avance II 400 MHz instrument at room temperature. Taking into account the molecular formula of the corresponding building blocks, one can then directly calculate the relative content of hydrophobic and hydrophilic block (for details see SI). The obtained values for the six different copolymers are summarised in Table 1, where the theoretically expected molar content is compared with that derived from the NMR spectra. In general, we find excellent agreement, which confirms that the monomers were incorporated in exactly the proportion added to the reaction mixture.

The number and weight average molecular weight and weight distribution of non-hydrolysed polymers were determined via gel permeation chromatography (GPC) using THF as eluent with a flow rate of 0.5 ml per minute at 25 °C (the GPC curves are shown in Fig. S6). The GPC was home-made with an isocratic pump and an autosampler (both from Thermo/Finnigan), a 3  $\mu$ m particle diameter front and 3  $\mu$ m

**Table 1** Relative molar content of hydrophobic and hydrophilic block according to the NMR spectra compared with the theoretically expected value. Theoretical molecular weight of hydrolysed polymer  $M_{th}$ , yield,experimental number average of the molecular weight ( $M_n$ ) of hydrolysed polymer and polydispersity index (PDI) from GPC experiments, and the experimentally determined chemical formula of the produced polymers

Theoretical formula	$nBu_{20}-b-AA_{100}$	$nBu_{40}-b-AA_{100}$	$nHex_{20}-b-AA_{100}$	$nDo_{20}-b-AA_{100}$	$nDo_{40}-b-AA_{100}$
h.phobic(%)	16.7	28.8	16.8	16.8	28.8
h.philic (%)	83.3	71.2	83.2	83.2	71.2
$M_{th}$ (g/mol)	9925	12,485	10,485	12,165	16,965
Experimental formula	$nBu_{40}-b-AA_{167}$	$nBu_{68}-b-AA_{167}$	$nHex_{37}-b-AA_{169}$	$nDo_{36}-b-AA_{127}$	$nDo_{36}-b-AA_{71}$
h.phobic(%)	19.5	29.0	18.1	22.0	33.8
h.philic(%)	80.5	71.0	83.2	78.0	66.2
Yield (%)	58	73	71	56	68
$M_n$ (g/mol)	17,181	20,681	17,681	17,681	13,953
PDI	1.15	1.19	1.12	1.20	1.28

particle diameter separation column (from PSS), as well as a refractive index detector (Wyatt Optilab DSP). The reference substance was a narrow distribution polystyrene standard.

Further information regarding the polymer composition was obtained via pH-titration (see Table S2 and Fig. S11) and the  $M_n$  and  $M_w$  results from GPC are given in Tables 1 and S1, and Fig. S6 shows monomodal and rather narrow distributions. In general, one finds that the polymers are larger by about 70% compared with the theoretical value, which would indicate that the initiation takes place only to a correspondingly reduced extent, i.e. a certain percentage of the initiator had become inactivated. In addition, it should be noted that GPC was done with a polystyrene standard (naturally no reference polymers are available for our copolymers), and accordingly, the absolute values for  $M_n$  and  $M_w$  might substantially deviate from the real values but are well comparable amongst each other. In this series only for the dodecyl polymer with the highest nDo content, some deviation is seen in a form of a shorter polymer, which would indicate that polymer growth is hindered here. The PDI values are between 1.1 and 1.2 as typically observed for ATRP, only being higher for the polymer with highest nDo content, which apparently from the polymerisation process was a bit more problematic (as also indicated by the GPC chromatogram that shows a shoulder at lower  $M_w$ ; Fig. S6).

## Methods of colloidal characterisation

The determination of the critical micelle concentration (cmc) was done by the fluorescence method [22]. For that purpose NaOH, stock solution was used in order to adjust the degree of deprotonation as 0.2 and 1.0 (20% excess of NaOH was added for the 1.0 solutions to ensure complete deprotonation). The weight percentage of polymer stock solutions was 10 g/L for both degrees of deprotonation. The polymer stock solutions

were then diluted to 11 different concentrations down to 0.05 mg/L using the pyrene stock solution.

Steady-state fluorescence spectra of pyrene were recorded with a Hitachi F-4500 Fluorescence Spectrometer at 25 °C from 350.0 to 420.0 nm after excitation at 334.0 nm. The slit width was set to 5.0 nm for both the excitation and the emission. For the experiments, a pyrene stock solution was prepared with a pyrene concentration of  $5 \times 10^{-8}$  mol/L.

The pH-titrations were performed at room temperature via a Titrand System with the Software tiamo™ by Metrohm.

Static light scattering (SLS) experiments were carried out with a CGS-3 (compact goniometer system) with a HeNe laser at 632.8 nm wavelength from ALV GmbH (Langen, Germany). Two avalanche photodiodes (APD) were used to detect the scattered light at various angles between 40 and 140°. The refractive index increment ( $dn/dc$ ) of the polymers was measured with the instrument Orange 19'' DN/DC.

The SLS intensity for particles should exhibit an angular dependence according to Guinier's law as follows:

$$I(q) = I(0) \cdot \exp(-R_g^2 \cdot q^2/3) \quad (1)$$

where  $R_g$  is the radius of gyration and  $q$  the modulus of the scattering vector ( $= 4\pi n_0 \sin(\theta/2)/\lambda$ ; with  $n_0$  the refractive index of the solvent,  $\theta$  the scattering angle and  $\lambda$  the wavelength of the light). From the intensity at zero angle,  $I(0)$ , one can, via the optical constant  $K$ , directly calculate the mass-averaged molecular weight  $M_w$  as follows:

$$M_w = I(0)/c \cdot K \quad (2)$$

$$K = 4 \frac{\pi^2 \cdot n_0^2 \cdot (dn/dc)^2}{N_{Av} \cdot \lambda^4} \quad (3)$$

where  $dn/dc$  is the refractive index increment and  $N_{Av}$  the Avogadro constant.

SANS measurements were performed at PA20 of the Laboratoire Léon Brillouin (LLB, Saclay, France). Three configurations were used with 1.9, 8.3 and 18.8 m sample-to-detector distances (SD) with a wavelength of 6 Å. In order to reach higher  $q$ , we used an off-centred detector position at the shortest detector distance, 1.9 m. Transmission values were measured in this configuration, in agreement with the existing measurement procedures (scripts) available at the instrument.

Some additional SANS measurements were performed on the V4 instrument at the Helmholtz Zentrum Berlin (HZB). The following three configurations were used: with SD and collimation (C) of SD = 1.35 m and C = 8 m, SD = 8 m and C = 8 m and SD = 15.60 m and C = 16 m. Two wavelengths of 4.5 and 12 Å (for SD = 15.60 m) were employed.

The coherent scattering intensity was obtained after normalisation of the detector cell efficiency using an incoherent scatterer (H<sub>2</sub>O), subtraction of the empty cell scattering and of the electronic noise (Cd). The scattering curve was obtained by isotropic regroupment with respect to the scattering centre, and taking into account the transmissions, the differential cross-sections were calculated [23]. All data evaluation was done by using the BerSANS software [24]. Subsequently, the data sets obtained for the three different configurations were merged. Finally, a constant background from the incoherent scattering was subtracted by extrapolating the intensity at large  $q$  by Porod's law [25] as the intensity here follows a  $q^{-4}$  behaviour.

## Results and discussion

### Critical micellar concentration (cmc)

A very important parameter describing the self-assembly properties of amphiphilic block copolymers in aqueous solution is their cmc. The cmc was determined by means of the fluorescence method where 0.05  $\mu\text{m}$  pyrene was employed as a probe molecule, and fluorescence spectra were measured in the block copolymer concentration range of 50  $\mu\text{g/L}$  to 5 g/L and are given in Fig. S12. Below the cmc, pyrene has to be located within an aqueous environment, while above it with large preference be contained in the hydrophobic core of the block copolymer micelles. This leads to a change of the fluorescence spectra, as for instance seen in the changing ratio of the first and third emission maximum ( $I_1/I_3$ ) [26]. From the ratio  $I_1/I_3$  ( $= I_{1/3}$ ) as a function of concentration one can determine the cmc. An example of such a plot is given in Fig. 3. The remaining such data sets are plotted in Fig. S13. The sigmoidal shape of the data sets was described by a Boltzmann-function as follows:

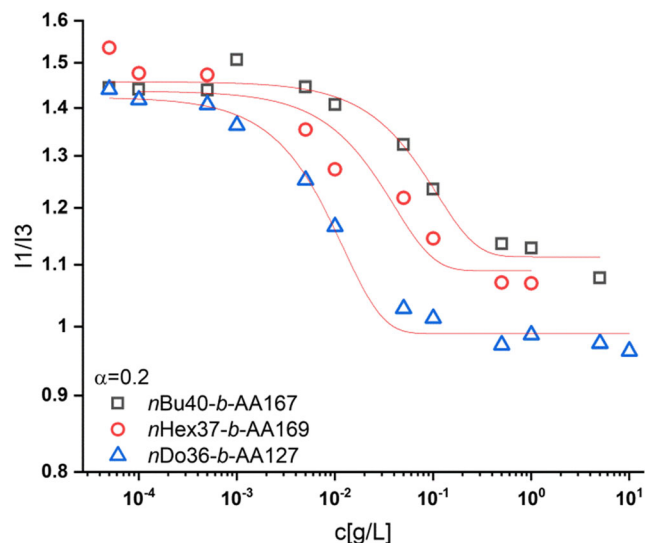


**Fig. 3** Ratio of the first and third maximum of the emission spectrum of pyrene as a function of concentration for the *nBu40-b-AA167*, *nHex37-b-AA169* and *nDo36-b-AA127* block copolymer and  $\alpha = 0.2$  ( $T = 25^\circ\text{C}$ )

$$I_{1/3} = I_{1/3f} + \frac{I_{1/3i} - I_{1/3f}}{1 + \exp((c - \text{cmc})/\Delta\text{cmc})} \quad (4)$$

with  $I_{1/3i}$  and  $I_{1/3f}$  being the initial (in pure water) and final ratio (presumably all in the micelles),  $c$  is the block copolymer concentration and  $\Delta\text{cmc}$  a measure for the width of the micellar transition regime. The cmc then is the inflexion point of these curves. The obtained cmc values are summarised in Table 2 and show only about a factor 20 difference between the most strongly hydrophobic block copolymer at lowest charging (*nDo36-b-AA71*,  $\alpha = 0.2$ ) and the least hydrophobic block copolymer at highest charging (*nBu40-b-AA167*,  $\alpha = 1.0$ ). It is interesting to note that the cmc becomes systematically lower with increasing length of the alkyl modification but depends less on the

**Table 2** CMC in M, as well as the corresponding free energy of micellisation  $\Delta G_{\text{mic}}$  for the different block copolymers at different degrees of ionisation  $\alpha$  at  $25^\circ\text{C}$

Polymer	$\alpha$	CMC [M]	$\Delta G_{\text{mic}}$ (kJ/mol)
<i>nBu40-b-AA167</i>	0.2	4.76E-06	-40.33
<i>nBu40-b-AA167</i>	1.0	6.51E-06	-39.55
<i>nBu68-b-AA167</i>	0.2	1.24E-06	-43.66
<i>nBu68-b-AA167</i>	1.0	4.04E-06	-40.73
<i>nHex37-b-AA169</i>	0.2	9.24E-07	-44.39
<i>nHex37-b-AA169</i>	1.0	1.38E-06	-43.39
<i>nDo36-b-AA127</i>	0.2	4.06E-07	-46.43
<i>nDo36-b-AA127</i>	1.0	7.00E-07	-45.08
<i>nDo36-b-AA71</i>	0.2	3.41E-07	-46.86
<i>nDo36-b-AA71</i>	1.0	4.20E-07	-46.35

block length (a reduction by a factor 2–3 seen for *n*Bu when going from 40 to 68 units). It might also be noted that a similar small decrease of cmc with increasing hydrophobic chain length has been observed for micelles of polybutadiene-*block*-poly (methacrylic acid) copolymers [11].

The change in Gibbs free energy ( $\Delta G_{\text{mic}}$ ) was calculated from the CMC data from the following equation:

$$\Delta G_{\text{mic}} = RT \ln x_{\text{CMC}} \quad (5)$$

where  $x_{\text{CMC}}$  is the critical micelle concentration expressed as mole fraction,  $T$  is the absolute temperature and  $R$  is the gas constant [27]. As the cmc changes, only little for the different block copolymers, correspondingly also, the Gibbs free energy of micellisation  $\Delta G_{\text{mic}}$  is changing only little, meaning that by going from butyl to dodecyl acrylate for about the same block length, the driving force for micelle formation increases by about 6 kJ/mol, i.e. much less than observed for increasing the chain length of a single chain surfactant by 8 methylene units! [28] Reducing the charge of the micelles by going from  $\alpha = 1.0$  to  $\alpha = 0.2$  in general leads to a change of  $\Delta G_{\text{mic}}$  by  $\sim 1.5$  kJ/mol, depending on the individual copolymer. For all dodecyl acrylate (Do) copolymers, cmc and  $\Delta G_{\text{mic}}$  are very close to each other, indicating that here the presence of the most hydrophobic alkyl chain dominates the properties.

Interestingly, the fluorescence measurements also yield further information regarding the polarity of the cores of the formed micelles. The observed final value of I1/I3 (see Fig. S13) becomes systematically lower in the series: *n*Bu40-*b*-AA167  $\rightarrow$  *n*Bu68-*b*-AA167  $\rightarrow$  *n*Hex37-*b*-AA169  $\rightarrow$  *n*Do36-*b*-AA127  $\rightarrow$  *n*Do36-*b*-AA71, exactly in line with the expected changes of polarity. The changes between the butyl block copolymers and the dodecyl block copolymers are marked, as expected since butyl and hexyl block copolymers apparently have a rather high polarity in their hydrophobic core.

### Static light scattering (SLS)

Static light scattering measurements were performed to gain a first insight into the aggregation behaviour of these block copolymers in aqueous solution. They were carried out for four different concentrations of 0.1, 0.2, 0.5 and 1.0 wt% with fully deprotonated samples ( $\alpha = 1.0$ ) in order to investigate concentration effect on these systems. Moreover, the samples with a concentration of 0.5 wt% were also measured for lower degree of deprotonation ( $\alpha = 0.2$ ). All SLS measurements were done in D<sub>2</sub>O.

SLS data was evaluated via Guinier plots for all block copolymers.  $I(0)$  values for all samples were obtained from these Guinier plots and  $M_w$  were calculated from these  $I(0)$  values, using the refractive index increment of the

corresponding polymer (see Table S3 for the  $dn/dc$  values). In particular, as hydrophobicity increases the calculated molecular weight of the aggregates increases as well. The obtained values are summarised in Fig. 4 and Table S4.

In general, it is observed that the obtained molecular weights are increasing with increasing concentration, but for the samples of *n*Bu<sub>68</sub>-*b*-AA<sub>167</sub> and the ones with dodecyl acrylate, this effect is small. Moreover, samples with dodecyl alkyl chain modification, which are the most hydrophobic ones, have much higher molecular weight values compared with other samples. Furthermore, when the pH-dependency of the systems is compared, it can be noticed that the  $M_w$  values do not differ largely between slightly and fully deprotonated samples, but the fully deprotonated samples form somewhat smaller aggregates, which can be explained via the packing parameter concept [9] according to which for a more highly charged head group one expects a larger head group area and correspondingly smaller spherical micelles are formed.

### Small-angle neutron scattering (SANS)

More detailed information regarding the structure of the micelles formed in aqueous solutions can be obtained from SANS experiments, systematically carried out for all block copolymers studied and for concentrations from 0.2, 0.5, up to 1.0 wt%. All SANS measurements were done in D<sub>2</sub>O for having good contrast conditions. The degree of ionisation was  $\alpha = 1.0$  for all concentrations and in addition  $\alpha$  values of 0.2 and 0.5 for the 0.5 wt% sample were studied.

The SANS patterns for almost all samples point to the formation of self-assembled aggregates. Only for Bu<sub>40</sub>-AA<sub>167</sub> and Hex<sub>37</sub>-AA<sub>169</sub>, the scattering is so low, especially

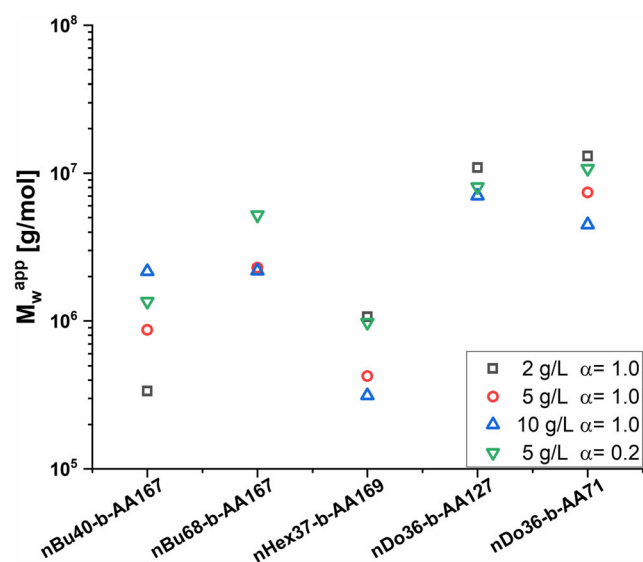


Fig. 4 Molecular weight as a function of the concentration for the different polymers studied ( $T = 25$  °C,  $\alpha = 1.0$ ; one measurement at  $\alpha = 0.2$ , 5 g/L) from SLS measurements at 25 °C

at lower concentration, which the pattern must arise from small and relatively open aggregates. The scattering intensity increases with increasing concentration for all samples (see Fig. S14) When comparing the scattering curves for the block copolymers of different length of the hydrophobic chain (Fig. 5), it is clearly seen that an increase in alkyl chain length is resulting in an increase of the scattering intensity, and the patterns at the same time become increasingly typical for globular aggregates. In other words, block copolymers with longer alkyl chain modification form bigger aggregates consistently. Even more obvious is the effect of the length of the hydrophobic block, where for the longer blocks much higher scattering intensities are seen, thereby indicating the formation of larger micelles.

Interestingly for the block copolymers having shorter alkyl side chains, i.e. Bu<sub>40</sub>-AA<sub>167</sub>, Bu<sub>68</sub>-AA<sub>167</sub> and Hex<sub>37</sub>-AA<sub>169</sub>, one also sees marked correlation peaks, presumably from electrostatic repulsion between the aggregates. The position of the correlation peak around 0.1 nm<sup>-1</sup> indicates a mean spacing between the aggregates of 50–60 nm, thereby corroborating the presence of aggregates with radii in the range of ~20 nm and aggregation numbers in the range of 30–100. For

Bu<sub>40</sub>-AA<sub>167</sub> which scatters least and shows rather low aggregation numbers at lowest concentration, the peak could also arise from chain–chain correlations, as they typically are observed in unscreened polyelectrolyte solutions [29, 30]. Interestingly for  $\alpha = 0.2$ , this peak is even more prominent, but here, the intensity is also 2–3 times higher, proving the presence of higher molecular mass. Such a correlation peak is not observed for the dodecyl analogues, and this is presumably due to the fact that the relatively higher molecular weight present has PAA chains extending into the surrounding solution and overlapping there, thereby reducing the effective repulsion.

Furthermore, it is interesting to compare in more detail the fully ( $\alpha = 1.0$ ) and little ( $\alpha = 0.2$ ) deprotonated samples. Samples of identical composition at full ionisation ( $\alpha = 1.0$ ) show lower scattering intensities than the corresponding samples at  $\alpha = 0.2$  (as seen before by static light scattering and for SANS in Fig. 5). Apparently, the aggregation number is getting smaller with increasing degree of ionisation. This effect is expected as the more charged head group of the polymeric amphiphile leads to a lower packing parameter and thereby to the lowering in the aggregation number and similar effects

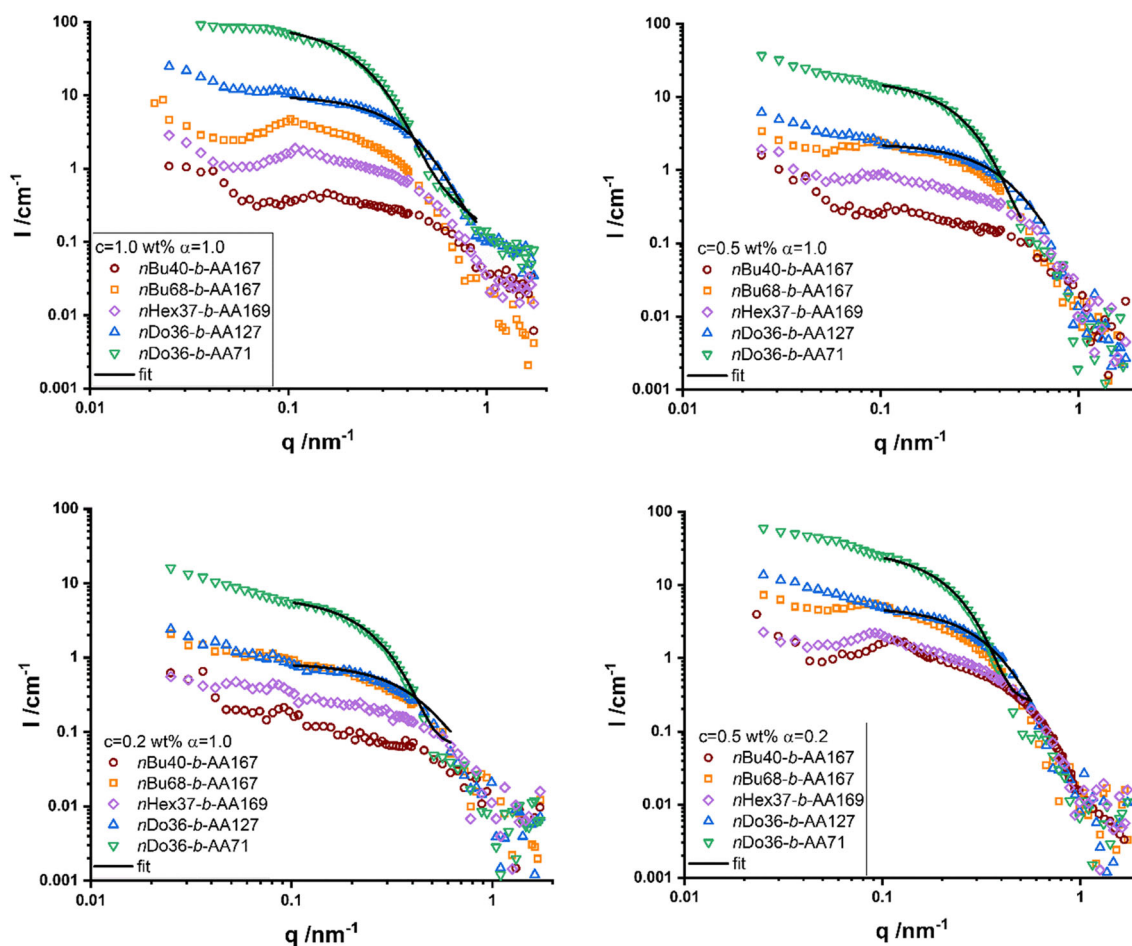


**Fig. 5** SANS intensity (corrected for the incoherent background) as a function of  $q$  for all samples with 0.2 to 1.0 wt% at  $\alpha = 1.0$ , and for 0.5 wt% also for  $\alpha = 0.2$  with fit curves for Guinier regime

have been seen before [31, 32]. The assembly is responding to such external stimuli, and such dynamic aggregation is often important for the properties of micellar assembly [33].

The results of a model-free analysis, employing the Guinier approximation and using the extrapolated intensity at zero angle  $I(0)$  to calculate the  $M_w$  (for details see SI), are summarised in Table S6, and the key parameter molecular weight  $M_w$  is shown in Fig. 6a for the variation of the total concentration and in Fig. 6b for the variation of the degree of ionisation (corresponding aggregation numbers are included in Table 3). In general, the tendencies seen here are very similar to those seen by light scattering (Fig. 4). Also, absolute numbers compare well, but on average are somewhat higher from light scattering, not surprising as there, due to the  $q$ -

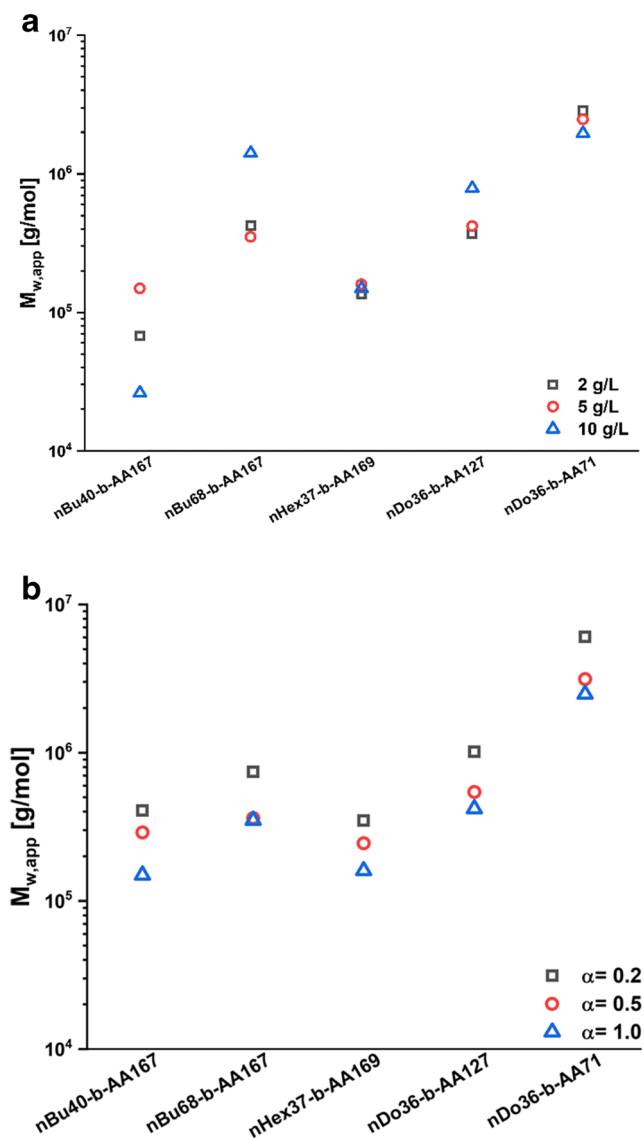


**Fig. 6** **a** Molecular weight as a function of the concentration for the different polymers studied ( $T=25^\circ\text{C}$ ,  $\alpha=1.0$ ). **b** Molecular weight as a function of the degree of ionisation  $\alpha$  for the different polymers studied ( $T=25^\circ\text{C}$ ,  $c=5\text{ g/L}$ )

range probed, the focus is more on larger structures.  $M_w$  and the aggregation number increase somewhat with increasing concentration. The increase is proportional to the hydrophobicity (length of the alkyl chain of the alkyl acrylate) but is mostly determined by the length of the hydrophobic block. Very marked is the effect of the degree of ionisation (Fig. 6b) where increased charging of the micelles leads to a reduction in size—as discussed before an expected trend when considering the packing parameter concept.

From these data, it becomes evident that nBu40-b-AA167 at full charging ( $\alpha=1.0$ ) forms only aggregates with  $N_{agg}$  of 4–9. Only at lower charging ( $\alpha=0.2$  or 0.5) real micelles with  $N_{agg}$  of 20–40 are formed, while at  $\alpha=1.0$  apparently, only a rather loose state of aggregation is present. This is substantially changed for nBu68-b-AA167, where micellar aggregates with  $N_{agg}$  in the range of 30–35 are observed even for full charging, which shows that the length of the hydrophobic block plays a crucial role for forming larger particles with higher molecular mass. The extension of the alkyl chain from butyl to hexyl for the short block length (Hex37-AA169) does lead to micellar aggregates of intermediate size. For the dodecyl case, nDo36-b-AA127 and nDo36-b-AA71, even for the lowest concentration and irrespective of the state of ionisation large globular micelles are observed, apparently due to a much larger degree of hydrophobicity. They are substantially larger by about a factor 8–10 in aggregation number for the shorter hydrophilic block (Table 3), where a smaller head group leads to aggregates with lower molecular weight. In general, it can be noted that only for the case of dodecyl acrylate really well-defined globular aggregates are formed, while apparently for the other block copolymers a simple core-corona model is not appropriate, as for instance seen by the further upturn of scattering intensity at low  $q$ . Accordingly, for nDo36-b-AA127 and nDo36-b-AA71, the aggregation numbers from SLS and SANS are in good agreement, while for the others the values from SLS are generally higher. This can be attributed to the fact that here apparently, the aggregates are less compacted and therefore one sees by SANS only structural subunits and lower aggregation numbers (as indicated by the further upturn of the scattering intensity at low  $q$ ).

As a next step, the SANS data was fitted for  $q > 0.1\text{ nm}^{-1}$  with a model of polydisperse spheres which were assumed to be composed of the hydrophobic block of the synthesised copolymers. This model is described by Eqs. 6 and 7, where  $\Delta\text{SLD}$  is the difference in scattering length densities between the hydrocarbon block and the average of the medium ( $\text{D}_2\text{O} + \text{PAA}$ ),  $R$  is the radius of the hydrophobic cores of the aggregates and  $q$  the magnitude of the scattering vector. A lognormal distribution (Eq. 8) was used to describe the polydispersity of the radius of the cores, with the width parameter  $\sigma$ ,  $R_m$  the mean radius and the number density  $N$  (fp), which is expressed as volume fraction fp, which can be defined using the Eq. 9 and

**Table 3** Molecular weight of the aggregates and aggregation numbers as derived from SLS and SANS for samples and for the concentrations of 2.0, 5.0, 10.0 g/L ( $\alpha = 1.0$ ) and for 5.0 g/L and  $\alpha = 0.2$ 

	Concentration (g/L)	SLS		SANS		Polymer
		$M_w^{\text{app}}$ (g/mol)	$N_{\text{agg}}$	$M_w^{\text{app}}$ (g/mol)	$N_{\text{agg}}$	
$\alpha = 1.0$	2	3.37E + 05	19.6	6.75E + 04	3.9	<b>nBu40-b-AA167</b>
	5	8.71E + 05	50.7	1.49E + 05	8.7	
	10	2.17E + 06	126.3	2.61E + 04	1.5	
$\alpha = 0.2$	5	1.36E + 06	79.0	4.07E + 05	23.7	
$\alpha = 1.0$	2	2.23E + 06	108.1	4.19E + 05	20.3	<b>nBu68-b-AA167</b>
	5	2.29E + 06	110.9	3.50E + 05	16.9	
	10	2.19E + 06	105.7	1.41E + 06	68.1	
$\alpha = 0.2$	5	5.22E + 06	252.2	7.44E + 05	36.0	
$\alpha = 1.0$	2	1.07E + 06	59.5	1.35E + 05	7.5	<b>nHex37-b-AA169</b>
	5	4.26E + 05	23.7	1.60E + 05	8.9	
	10	3.15E + 05	17.5	1.48E + 05	8.3	
$\alpha = 0.2$	5	9.77E + 05	54.4	3.49E + 05	19.4	
$\alpha = 1.0$	2	1.09E + 07	610.6	3.67E + 05	20.5	<b>nDo36-b-AA127</b>
	5	7.64E + 05	42.8	4.19E + 05	23.4	
	10	7.01E + 06	392.4	7.85E + 05	43.9	
$\alpha = 0.2$	5	8.07E + 06	452.0	1.01E + 06	56.8	
$\alpha = 1.0$	2	1.30E + 07	934.8	2.85E + 06	204.3	<b>nDo36-b-AA71</b>
	5	7.39E + 06	529.6	2.47E + 06	177.3	
	10	4.49E + 06	321.6	1.96E + 06	140.6	
$\alpha = 0.2$	5	1.07E + 07	770.1	6.05E + 06	433.3	

Eq. 10. In that formula,  $\langle R^3 \rangle$  is the third moment of the lognorm distribution of the radii.

$$I(q, R_m) = {}^1 N(fp) \int_0^\infty \text{LogNorm}(R, N(fp), \sigma, R_m) F(q, R) dR \quad (6)$$

$$F(q, R) = \left( \frac{4\pi R^3 \Delta \text{SLD} (\sin(qR) - qR \cos(qR))}{(qR)^3} \right)^2 \quad (7)$$

$$\text{lognorm}(R, N(fp), \sigma, R_m) = \frac{N(fp)}{R} \exp\left(\frac{-\ln(R/R_m)^2}{2\sigma^2}\right) \quad (8)$$

$${}^1 N(fp) = \frac{fp^3}{4\pi \langle R^3 \rangle} \quad (9)$$

$$\langle R^3 \rangle = R_m^3 \exp\left(\frac{9}{2} \sigma^2\right) \quad (10)$$

We considered only the hydrophobic block for the calculation of the contrast ( $\Delta \text{SLD}$ ), which was calculated as  $61.5 \cdot 10^9 \text{ cm}^{-2}$  for nDo containing polymers. The PAA part of the polymers was counted as being part of the solvent as the stretched length of the PAA block is about 25 nm and therefore should be homogeneously distributed between the hydrophobic cores of the aggregates.

This analysis was only done for the nDo polymers as only here the scattering patterns showed nicely the features of compact spherical structures. From the quantitative analysis of the scattering data with a model of homogenous sphere, it can be concluded that the core radius of the aggregates increases with decreasing length of the hydrophilic block (Table S7,  $R_m$  values correspond to the value arising from the hydrophobic domains). The ratio between fitted and calculated volume fraction  $fp/\Phi$  gives an idea about how large the tendency for hydrophobic aggregation is. The ratio is getting closer to 1 for increasing concentrations, thereby confirming complete aggregation of the block copolymer and self-consistency of the model.

The fits are generally in quite good agreement with the experimental data (see Figs. 5 and S17) and the derived parameters agree well with model-free analysis (Table 3). This then confirms the model of having well-defined, homogeneous spherical micelles for the case of nDo as hydrophobic block, while more open and less compacted structures are formed for butyl and hexyl acrylate.

Especially for the dodecyl copolymers, the scattering patterns indicate the presence of well-defined spherical aggregates, thereby allowing to deduce the head group areas  $a_h$  (as the interface per molecule on the surface of the hydrophobic core,  $a_h = 4\pi R_c^2 / N_{\text{agg}}$ ) and interpret data within the

geometric packing parameter concept [14]. If one calculates  $a_h$  for *nDo36-b-AA127* at 5 g/L and  $\alpha = 1.0$ , one obtains a value of 15.1 nm<sup>2</sup>, which becomes reduced to 11.2 nm<sup>2</sup> for  $\alpha = 1.0$ . This indicates a substantially larger head group due to the enhanced electrostatic repulsion for full charging of the carboxylate units. For the *nDo36-b-AA71* the corresponding values for  $a_h$  would be 6.5 and 4.8 nm<sup>2</sup>, respectively, confirming this reduction by reduced electrostatic repulsion but much more marked is here the effect of shortening the length of the polyelectrolyte (PAA) head group.

## Conclusions

In this work, a number of different amphiphilic block copolymers of the type poly (alkyl acrylate)-*b*-poly (acrylic acid) (PAlkA-*b*-PAA) have been synthesised. The hydrophilic block had always around 100 units of acrylic acid, while the hydrophobic block had a length of 35–70 units. Its hydrophobicity was varied by employing butyl, hexyl and dodecyl acrylate thereby increasing the hydrophobic character of the formed micellar core. The self-assembly of these amphiphilic block copolymers was studied in aqueous solution, where the degree of ionisation of the PAA block was varied from 20 to 100%. The determination of the critical micelle concentration (cmc) by a fluorescence method showed only a small effect of the block copolymer architecture, but along the expected trends, i.e. the cmc increased with higher ionisation of the PAA, shorter hydrophobic blocks and shortening the alkyl chain of the alkyl acrylate.

The structure of their micellar aggregates in dilute aqueous solution was studied by a combination of static light scattering (SLS) and small-angle neutron scattering (SANS). Here, it was seen that the mass of the aggregates depends largely on the length of the alkyl chain and only for dodecyl acrylate large and well-defined micelles with aggregation numbers of above 100 are formed. In contrast, for the shortest chain of butyl acrylate (Bu<sub>40</sub>) only lower molar mass are seen by SANS, with which their low aggregation number cannot be proper micelles, while SLS shows significantly higher Mw values. Apparently, here, no compacted micellar structures are present, but rather loose aggregates that interconnect to a larger superstructure. Upon lengthening the hydrophobic block, the micelles become much bigger, while the change from butyl acrylate to hexyl acrylate has only a smaller influence. In all cases, a marked effect of the degree of ionisation is observed, where for higher charging, the mass becomes smaller, in good agreement with the packing parameter concept; as for high charging, the hydrophilic block should require a larger head group area at the interface.

In summary, it can be stated that by variation of the type and length of the hydrophobic block in block copolymers of PAlkA-*b*-PAA one can control the aggregation state in

solution over a wide range. This is interesting as in addition, one can expect that the solubilisation properties of the hydrophobic block should also depend largely on the length of the alkyl chain of alkyl acrylate, a topic that is to be explored in detail in future research.

**Acknowledgements** The authors are grateful to Jana Lutzki for dn/dc measurements, to Sebastian Bayer and Anja Hörmann for SANS measurements and data reduction, to the Helmholtz-Zentrum Berlin (HZB) für Materialien und Energie GmbH (HZB, Berlin, Germany) and the Laboratoire Léon Brillouin (LLB, Saclay, France) for allocation of SANS beam time. In particular, we would like to thank Uwe Keiderling from HZB for the help with the SANS measurements. Furthermore, we thank the research group of Prof. Schlaad from University of Potsdam for performing the GPC measurements.

**Funding information** Open Access funding provided by Projekt DEAL. We would like to thank Technische Universität Berlin for the financial support.

**Open Access** This article is licensed under a Creative Commons Attribution 4.0 International License, which permits use, sharing, adaptation, distribution and reproduction in any medium or format, as long as you give appropriate credit to the original author(s) and the source, provide a link to the Creative Commons licence, and indicate if changes were made. The images or other third party material in this article are included in the article's Creative Commons licence, unless indicated otherwise in a credit line to the material. If material is not included in the article's Creative Commons licence and your intended use is not permitted by statutory regulation or exceeds the permitted use, you will need to obtain permission directly from the copyright holder. To view a copy of this licence, visit <http://creativecommons.org/licenses/by/4.0/>.

## References

- Gohy J-F (2005) Block copolymer micelles BT - block copolymers II. In: Abetz V (ed). Springer Berlin Heidelberg, Berlin, Heidelberg, pp 65–136
- Förster S, Abetz V, Müller AHE (2004) Polyelectrolyte block copolymer micelles. In: Polyelectrolytes with Defined Molecular Architecture II. pp 173–210
- Yu K, Eisenberg A (1996) Multiple morphologies in aqueous solutions of aggregates of polystyrene-block-poly (ethylene oxide) diblock copolymers. *Macromolecules* 29:6359–6361. <https://doi.org/10.1021/ma960381u>
- Poppe A, Willner L, Allgaier J, Stellbrink J, Dieter R (1997) Structural investigation of micelles formed by an amphiphilic PEP-PEO block copolymer in water. *Macromolecules* 30:7462–7471. <https://doi.org/10.1021/ma970470m>
- Boschetti-de-Fierro A, Müller AJ, Abetz V (2007) Synthesis and characterization of novel linear PB-*b*-PS-*b*-PEO and PE-*b*-PS-*b*-PEO triblock terpolymers. *Macromolecules* 40:1290–1298. <https://doi.org/10.1021/ma0625713>
- Jensen GV, Shi Q, Deen GR, Almdal K, Pedersen JS (2012) Structures of PEP-PEO block copolymer micelles: effects of changing solvent and PEO length and comparison to a thermodynamic

- model. *Macromolecules* 45:430–440. <https://doi.org/10.1021/ma2016369>
7. Kataoka K, Harada A, Nagasaki Y (2012) Block copolymer micelles for drug delivery: design, characterization and biological significance. *Adv Drug Deliv Rev* 64:37–48. <https://doi.org/10.1016/j.addr.2012.09.013>
  8. Cabral H, Miyata K, Osada K, Kataoka K (2018) Block copolymer micelles in nanomedicine applications. *Chem Rev* 118:6844–6892. <https://doi.org/10.1021/acs.chemrev.8b00199>
  9. Glass R, Möller M, Spatz JP (2003) Block copolymer micelle nanolithography. *Nanotechnology* 14:1153–1160. <https://doi.org/10.1088/0957-4484/14/10/314>
  10. Shen H, Eisenberg A (2000) Control of architecture in block-copolymer vesicles. *Angew Chemie - Int Ed* 39:3310–3312. [https://doi.org/10.1002/1521-3773\(20000915\)39:18<3310::AID-ANIE3310>3.0.CO;2-2](https://doi.org/10.1002/1521-3773(20000915)39:18<3310::AID-ANIE3310>3.0.CO;2-2)
  11. Fernyhough C, Ryan AJ, Battaglia G (2009) PH controlled assembly of a polybutadiene-poly (methacrylic acid) copolymer in water: packing considerations and kinetic limitations. *Soft Matter* 5:1674–1682. <https://doi.org/10.1039/b817218h>
  12. Riemer S, Prévost S, Dzionara M, Appavou MS, Schweins R, Gradzielski M (2015) Aggregation behaviour of hydrophobically modified polyacrylate – variation of alkyl chain length. *Polymer* 70:194–206. <https://doi.org/10.1016/j.polymer.2015.06.010>
  13. Hamley IW (2005) Nanoshells and nanotubes from block copolymers. *Soft Matter* 1:36–43. <https://doi.org/10.1039/b418226j>
  14. Israelachvili JN, Mitchell DJ, Ninham BW (1977) Theory of self-assembly of lipid bilayers and vesicles. *BBA - Biomembr* 470:185–201. [https://doi.org/10.1016/0005-2736\(77\)90099-2](https://doi.org/10.1016/0005-2736(77)90099-2)
  15. Gillies ER, Fréchet JMJ (2004) Development of acid-sensitive copolymer micelles for drug delivery. *Pure Appl Chem* 76:1295–1307. <https://doi.org/10.1351/pac200476071295>
  16. Rutkaite R, Swanson L, Li Y, Armes SP (2008) Fluorescence studies of pyrene-labelled, pH-responsive diblock copolymer micelles in aqueous solution. *Polymer* 49:1800–1811. <https://doi.org/10.1016/j.polymer.2008.02.007>
  17. Nicolai T, Colombani O, Chassenieux C (2010) Dynamic polymeric micelles versus frozen nanoparticles formed by block copolymers. *Soft Matter* 6:3111–3118. <https://doi.org/10.1039/b925666k>
  18. Hickl P, Ballauff M, Jada A (1996) Small-angle X-ray contrast-variation study of micelles formed by poly (styrene)-poly (ethylene oxide) block copolymers in aqueous solution. *Macromolecules* 29:4006–4014. <https://doi.org/10.1021/ma951480v>
  19. Fox ME, Szoka FC, Fréchet JMJ (2009) Soluble polymer carriers for the treatment of cancer: the importance of molecular architecture. *Acc Chem Res* 42:1141–1151. <https://doi.org/10.1021/ar900035f>
  20. Colombani O, Ruppel M, Schubert F, Zettl H, Pergushov DV, Müller AHE (2007) Synthesis of poly(*n*-butyl acrylate)-block-poly (acrylic acid) diblock copolymers by ATRP and their micellization in water. *Macromolecules* 40:4338–4350. <https://doi.org/10.1021/ma0609578>
  21. Petrov PD, Drechsler M, Müller AHE (2009) Self-assembly of asymmetric poly (ethylene oxide)-block-poly(*n*-butyl acrylate) diblock copolymers in aqueous media to unexpected morphologies. *J Phys Chem B* 113:4218–4225. <https://doi.org/10.1021/jp809598v>
  22. Le Zhao C, Winnik MA, Riess G, Croucher MD (1990) Fluorescence probe techniques used to study micelle formation in water-soluble block copolymers. *Langmuir* 6:514–516. <https://doi.org/10.1021/la00092a038>
  23. Chen SH, Lin TL (1987) Colloidal solutions. *Methods Exp Phys* 23:489–543
  24. Keiderling U (2002) The new “BerSANS-PC” software for reduction and treatment of small angle neutron scattering data. *Appl Phys A Mater Sci Process* 74:1455–1457. <https://doi.org/10.1007/s003390201561>
  25. Glatter O, Kratky O (1982) Small angle x-ray scattering. Academic Publisher, London
  26. Wilhelm M, Zhao CL, Wang Y, Xu R, Winnik MA (1991) Poly (styrene-ethylene oxide) block copolymer micelle formation in water: a fluorescence probe study. *Macromolecules* 24:1033–1040. <https://doi.org/10.1021/ma00005a010>
  27. Rosen MJ, Kunjappu JT (2012) Micelle formation by surfactants. *Surfactants and interfacial phenomena*. Wiley, Hoboken, pp 123–201
  28. Klevens HB (1953) Structure and aggregation in dilute solution of surface active agents. *J Am Oil Chem Soc* 30:74–80. <https://doi.org/10.1007/BF02635002>
  29. Kaji K, Urakawa H, Kanaya T, Kitamaru R (1988) Phase diagram of polyelectrolyte solutions. *J Phys* 49:993–1000. <https://doi.org/10.1051/jphys:01988004906099300>
  30. Combet J, Lorchat P, Rawiso M (2012) Salt-free aqueous solutions of polyelectrolytes: small angle X-ray and neutron scattering characterization. *Eur Phys J Spec Top* 213:243–265. <https://doi.org/10.1140/epjst/e2012-01674-3>
  31. Burkhardt M, Martinez-Castro N, Tea S, Drechsler M, Babin I, Grishagin I, Schweins R, Pergushov DV, Gradzielski M, Zezin AB, Müller AHE (2007) Polyisobutylene-block-poly (methacrylic acid) diblock copolymers: self-assembly in aqueous media. *Langmuir* 23:12864–12874. <https://doi.org/10.1021/la701807b>
  32. Pergushov DV, Remizova EV, Gradzielski M, Lindner P, Feldthusen J, Zezin AB, Müller AHE, Kabanov VA (2004) Micelles of polyisobutylene-block-poly (methacrylic acid) diblock copolymers and their water-soluble interpolyelectrolyte complexes formed with quaternized poly(4-vinylpyridine). *Polymer* 45:367–378. <https://doi.org/10.1016/j.polymer.2003.10.086>
  33. Gradzielski M (2004) Investigations of the dynamics of morphological transitions in amphiphilic systems. *Cur Opin Colloid Interface Sci* 9:256–263. <https://doi.org/10.1016/j.cocis.2004.05.032>

**Publisher's note** Springer Nature remains neutral with regard to jurisdictional claims in published maps and institutional affiliations.



**Özge Azeri** was born in 1988 in Istanbul, studied Chemistry at the Middle East Technical University in Ankara/Turkey and received her bachelor's and master's degrees there. As a bachelor and master student, she worked on the synthesis of conjugated polymers for Organic Photovoltaic applications with Prof. Cirpan. During her master's study in Turkey, she was awarded a scholarship for her further studies from the Ministry of National Education of the Republic of Turkey. Since 2017, she is a Ph.D. candidate at the Technische Universität Berlin, Germany with Prof. Gradzielski. Her Ph.D. research is concerned with the synthesis and characterization of amphiphilic copolymers and the investigation of their colloidal systems.



**Dennis Schönfeld** was born in 1990 in Berlin and passed his education as a certified chemical-technical assistant there. He studied applied chemistry in Aachen, Germany and received his bachelor's degree with distinction in 2015. At the Technische Universität Berlin, Germany, he continued his studies and obtained the M.Sc. graduation in 2018. During his master's study, his research was concerned with the synthesis and characterization of amphiphilic copolymers with Prof.

Gradzielski. Since 2018, he is a Ph.D. candidate at the Fraunhofer Institute for Applied Polymer Research, Potsdam-Golm, Germany. Particularly, his research work is focusing on the synthesis, blending and characterization of functional shape memory polymers.



**Laurence Noirez** is CNRS Research Director at the Léon Brillouin Laboratory (CEA-CNRS), Université Paris-Saclay (France). She received the Degree of Doctor of Science from the Université Paris XI in 1989 and holds a Habilitation to conduct researches from the Université Paris IV since 1998. Dr. Noirez holds also an Engineering Diploma with a specialization in High Polymers from the Université Louis Pasteur (Strasbourg). She was appointed

member of the CoNRS (2012-2016), member of the Agence Nationale de la Recherche (2013-2017), and is currently co-coordinator of a European project ITN H2020. Her recent thematic programs developed relate to the understanding of collective effects in fluids. The subjects covered include the structural, dynamic, optical, magnetic and microthermal study of common and complex fluids. Dr L. Noirez has established that liquids are long range elastically correlated and measured their "static" shear elasticity. She also highlighted the impact of interfacial forces, and showed that the temperature of liquids can be modulated by a

mechanical excitation. She contributes to scientific collaborative national and international programs and is also involved in instrumental neutron scattering programs.



**Michael Gradzielski** was born in 1962 in Bayreuth, studied chemistry at the Universität Bayreuth, Germany and received his PhD there in 1992. In between, he stayed in 1985/1986 as a Fulbright scholar at the University of Wisconsin—Madison and obtained a MSc in chemistry. After a post-doctoral stay at the Laboratoire de Physique Statistique at the Ecole Normale Supérieure, Paris (Prof. D. Langevin), he finished his habilitation for Physical Chemistry at the

Universität Bayreuth in 2000. Since 2004, he is a full professor for Physical Chemistry at the Technische Universität Berlin, Germany. In addition, he has been a visiting scientist at the Institut Laue-Langevin (ILL), Grenoble (France) and a visiting professor at Doshisha University, Kyoto (Japan). He has been a dean of the Faculty of Mathematics and Natural Sciences of the TU Berlin from 2014 to 2017, and since 2019, he is the president of the Kolloid-Gesellschaft. His research work is concerned with the investigation of colloidal systems with an emphasis on their structural characterisation and structure-property relations. Particular fields of interest here are surfactants and amphiphilic copolymers, micelles, microemulsions, solubilisation, vesicles and properties of nanoparticles.